Cell Host & Microbe
Article

Kinesin-1-Mediated Capsid Disassembly and Disruption of the Nuclear Pore Complex Promote Virus Infection

Sten Strunze,[1,3] Martin F. Engelke,[1,3] I-Hsuan Wang,[1] Daniel Puntener,[1] Karin Boucke,[1] Sibylle Schleich,[2] Michael Way,[2] Philipp Schoenenberger,[1] Christoph J. Burckhardt,[1,4] and Urs F. Greber[1,*]
[1]Institute of Molecular Life Sciences, University of Zürich, Winterthurerstrasse 190, CH-8057 Zürich, Switzerland
[2]Cancer Research UK, 407 St. John Street, Lincoln's Inn Field, London EC1V 4AD, UK
[3]These authors contributed equally to this work
[4]Present address: Department of Cell Biology, Harvard Medical School, 240 Longwood Avenue, Boston, MA 02115, USA
*Correspondence: urs.greber@imls.uzh.ch
DOI 10.1016/j.chom.2011.08.010

SUMMARY

Many viruses deliver their genomes into the host cell nucleus for replication. However, the size restrictions of the nuclear pore complex (NPC), which regulates the passage of proteins, nucleic acids, and solutes through the nuclear envelope, require virus capsid uncoating before viral DNA can access the nucleus. We report a microtubule motor kinesin-1-mediated and NPC-supported mechanism of adenovirus uncoating. The capsid binds to the NPC filament protein Nup214 and kinesin-1 light-chain Klc1/2. The nucleoporin Nup358, which is bound to Nup214/Nup88, interacts with the kinesin-1 heavy-chain Kif5c to indirectly link the capsid to the kinesin motor. Kinesin-1 disrupts capsids docked at Nup214, which compromises the NPC and dislocates nucleoporins and capsid fragments into the cytoplasm. NPC disruption increases nuclear envelope permeability as indicated by the nuclear influx of large cytoplasmic dextran polymers. Thus, kinesin-1 uncoats viral DNA and compromises NPC integrity, allowing viral genomes nuclear access to promote infection.

INTRODUCTION

In eukaryotic cells, transport between the nucleus and the cytoplasm during interphase is controlled by the nuclear pore complex (NPC). The NPC is a supramolecular assembly of at least 30 different proteins (Alber et al., 2007; D'Angelo and Hetzer, 2008). It is anchored in the nuclear envelope by several transmembrane nucleoporins (Nups). Membrane-proximal scaffolding Nups maintain the framework of the NPC, while central and peripheral phenylalanine-glycine (FxFG and GLFG)-rich Nups provide a selective phase barrier, which controls passive diffusion and facilitated transport of macromolecules through the NPC. The NPC has barrier and transport functions, with cargo size restriction of about 39 nm for receptor-mediated transport and solutes of about 40 kD (Mohr et al., 2009; Pante and Kann, 2002). FG-repeat-containing peripheral Nups including Nup358 (also referred to as RanBP2) and Nup153 are predicted to form a noncohesive dynamic network based on a higher fraction of charged amino acid residues between FG domains compared to the cohesive Nups and thereby act as an entropic barrier (Lim et al., 2007; Patel et al., 2007; Ribbeck and Gorlich, 2002). Proteins and nucleic acids bound to import or export receptors are transported through the NPC by a facilitated mechanism involving cumulative reversible steps on natively unfolded FxFG- and GLFG-rich Nups and a final irreversible exit step (Frey and Gorlich, 2007; Lowe et al., 2010). NPCs of mammalian cells are largely immobile, but their peripheral proteins can have short residence times of seconds to minutes, suggesting that NPC substructures are highly dynamic and may have multiple functions (Daigle et al., 2001). For example, NPCs dynamically interact with chromatin, thereby controlling genome organization and gene expression. They also recruit motor proteins, such as dynein-dynactin, which binds to Nup358 of the cytoplasmic NPC filaments in the G2 phase of the cell cycle (Splinter et al., 2010), or kinesin-1 throughout interphase (Cai et al., 2001). NPC malfunction or mutations in Nups have been associated with human pathologies, including cancer and cardiac diseases (Zhang et al., 2008). As we age, NPCs also become leaky due to oxidative damage and proteasome-mediated degradation of the stable NPC-resident scaffolding Nups (D'Angelo et al., 2009).

The size restriction of normal NPCs precludes most viral capsids from directly accessing the nucleus (reviewed in Puntener and Greber, 2009; Suzuki and Craigie, 2007). Yet certain viruses deliver their genome into the nucleus and uncoat in the cytoplasm. Nuclear import of reverse transcribed HIV preintegration complex, for example, is restricted by cellular factors binding to the viral capsid and depends on Nups, in particular the FG-containing Nup153 (Lee et al., 2010; Woodward et al., 2009). Herpesviruses dock to the NPC predominantly by Nup214 (Copeland et al., 2009; Pasdeloup et al., 2009) and are thought to import DNA using a pressure-based mechanism (Newcomb et al., 2001). Adenoviruses are also critically dependent on nuclear import of their genome. They cause respiratory, gastrointestinal, urogenital, and ocular disease with epidemic potential and occasionally fatal outcomes (Hayashi and Hogg, 2007; Kojaoghlanian et al., 2003). Human adenovirus type 2/5

(HAdV-2/5, short Ad2/5) enters polarized epithelial cells by triggering a cytokine response from macrophages, which leads to relocation of the coxsackievirus Ad receptor CAR and integrin coreceptors to the apical plasma membrane (Lutschg et al., 2011). The virus subsequently exposes the viral lytic factor protein VI (Wiethoff et al., 2005) by using CAR receptor drifts and integrin confinements (Burckhardt et al., 2011). Cytosolic particles engage in bidirectional microtubule-based transport to the nucleus (Bremner et al., 2009; Gazzola et al., 2009; Suomalainen et al., 1999), dock to the NPC protein Nup214, and attach the highly mobile nuclear histone H1 to acidic clusters of the major capsid protein hexon (Rux and Burnett, 2000; Trotman et al., 2001). Viral capsids are disassembled by an unknown mechanism at the NPC, as revealed by a conformation-specific anti-hexon antibody or the dissociation of the internal core protein pV in case of a transgenic Ad2-GFP-pV (Puntener et al., 2011). Capsid fragments are left behind in the cytoplasm (Greber et al., 1997; Martin-Fernandez et al., 2004), and consequently, viral DNA enters the nucleus (Greber et al., 1997). Here, we found that the anterograde microtubule motor kinesin-1 disrupts NPC-docked capsids and surprisingly also the NPC, and opens access for the viral genome into the nucleus.

RESULTS

Disassembled Viral Capsids in the Cytoplasm Are Associated with Nucleoporins

Immunofluorescence analysis of cells infected with Texas red (TR)-labeled Ad2 particles using a polyclonal anti-capsid antibody (R70), which specifically detects disrupted but not intact Ad2 capsids after DNA import into the nucleus (see Figure S1A available with this article online, and Puntener et al., 2011; Trotman et al., 2001), reveals that the cell periphery is enriched in numerous R70-postive puncta at 180 min postinfection (p.i.) (Figure 1A). Thin-section transmission electron microscopy (TEM) of infected cells at 180 min p.i. showed that cytosolic viral structures were significantly reduced in size compared to intact particles at the plasma membrane, or partly disrupted particles in endosomes 7 min p.i. (Figures 1B and 1C). These structures often occurred in clusters and appeared as disrupted capsid clusters, indicated by correlative fluorescence microscopy and TEM (Figure S1Ab). Since capsid disassembly occurs at the NPC (Trotman et al., 2001), we tested if these viral puncta were positive for Nups. By confocal microscopy, we found Nup358, Nup214, and Nup62, but not Nup153, on amorphous cytosolic capsid puncta, irrespective of whether the cells were treated with the protein synthesis inhibitor cycloheximide (Figures 1D and 1E). The capsids of a virus mutant Ad5-ΔpIX, which lacked the small capsid protein IX (pIX), were transported in the cytoplasm as wild-type virus (Gazzola et al., 2009), and had strongly reduced Nup358 and Nup62 signals, demonstrating that these Nups did not just randomly associate with the major capsid protein hexon (see Figure 1E and Figures S1Ba and S1Bb). Noninfected cells or cells infected for less than 60 min had no detectable Nups in the cell periphery (Figure S1Bc, data not shown). Similar to Nup358, Nup214, and Nup62, which occur in a complex (reviewed in Suntharalingam and Wente, 2003), the Nup358 binding protein RanGAP1 (Mahajan et al., 1997), and the nuclear export factor Crm1, which binds to Nup214 and Nup358 during nuclear export (Bernad et al., 2004; Hutten and Kehlenbach, 2006), localized to peripheral cytoplasmic Ad2 particles at 180 min p.i. (Figures S1Bd and S1C, Movie S1). There was no evidence for Nup proteolysis by western blot analyses of infected cell extracts (data not shown), suggesting that Nup colocalization with disrupted cytoplasmic Ad is not related to apoptotic proteolysis. None of the Nups tested, nor RanGAP1 or Crm1, however, were found on viruses in cells treated with the Crm1 inhibitor leptomycin B (LMB), which blocks nuclear export and prevents viral localization to the nucleus (Figure S1Be). Importantly, LMB blocked not only the appearance of R70 epitopes but also the dissociation of the capsid protein GFP-pV from the viruses, indicating that it blocked capsid disassembly (Puntener et al., 2011; Strunze et al., 2005).

To examine if the recruitment of Nups and associated proteins to disrupted cytosolic Ad2 capsids occurred upon contact of the virus with the NPC at the nuclear envelope, we expressed the photoconvertible Kaede-Nup214 in HeLa cells for 48 hr. Nup214 is one of the most stable Nups, with an estimated NPC residence time of about 40 hr (Daigle et al., 2001; Rabut et al., 2004). Kaede-Nup214 was incorporated into the nuclear envelope in a punctate pattern typical for NPCs (Figure S1Da). Cells expressing Kaede-Nup214 were inoculated with Ad2-atto647 and the nucleus photoactivated with 355 plus 405 nm light, according to previously described protocols (Ando et al., 2002). Nonconverted Kaede-Nup214, converted Kaede-Nup214, and virus capsid fluorescence were imaged at 488, 561, and 633 nm excitation, respectively, at 90–160 min p.i. (Figure 1F). From about 3000 analyzed viruses and 59 virus clusters (defined by a thresholding algorithm, see Figure S1Db), we found ten events of converted Kaede-Nup214 colocalization with clustered Ad2-atto647 (Figure 1F, arrows; 17% positive clusters, Figure 1G) and none with nonclustered Ad2-atto647, while nonconverted Kaede-Nup214 colocalized with estimated less than 1% of nonclustered Ad2-att647 (Figure 1F, double arrowheads). These data indicate a functional relationship between clustered (aggregated, disassembled) capsids in the cytosol and Kaede-Nup214 at the nuclear envelope.

Viral Capsid Disruption Requires Kinesin-1

Live-cell analyses of Crm1-GFP-expressing cells revealed Crm1-GFP-positive Ad2 capsids in trajectories from the nuclear envelope to the periphery, reminiscent of microtubule-dependent motions (see Figure S1C, Movie S1). We examined whether disassembled capsids colocalized with kinesin-1 given the localization of viruses in the cell periphery, and the role of this anterograde microtubule motor in moving cellular and viral cargos, including vaccinia virus, African swine fever virus, and herpesviruses from the cell center to the periphery (reviewed in Greber and Way, 2006). We found that cytosolic capsid aggregates in the cell periphery were positive for kinesin light-chain 1 (Klc1) as well as Klc2-GFP (Figures 2A and 2B). GFP-Klc2 was observed on motile Ad2-TR viruses moving in a linear and continuous fashion at μm/s velocities from the cell center to the periphery at 239 min p.i., when most of the Ad2-TR particles were positive for Klc2-GFP (Movie S2). This is consistent with the observed speeds for kinesin-1 in single molecule studies (Watanabe et al., 2010).

The N terminus of KLC1/2 is predicted to engage in coiled-coil interactions with the heavy chain of Kif5 (Mandelkow and

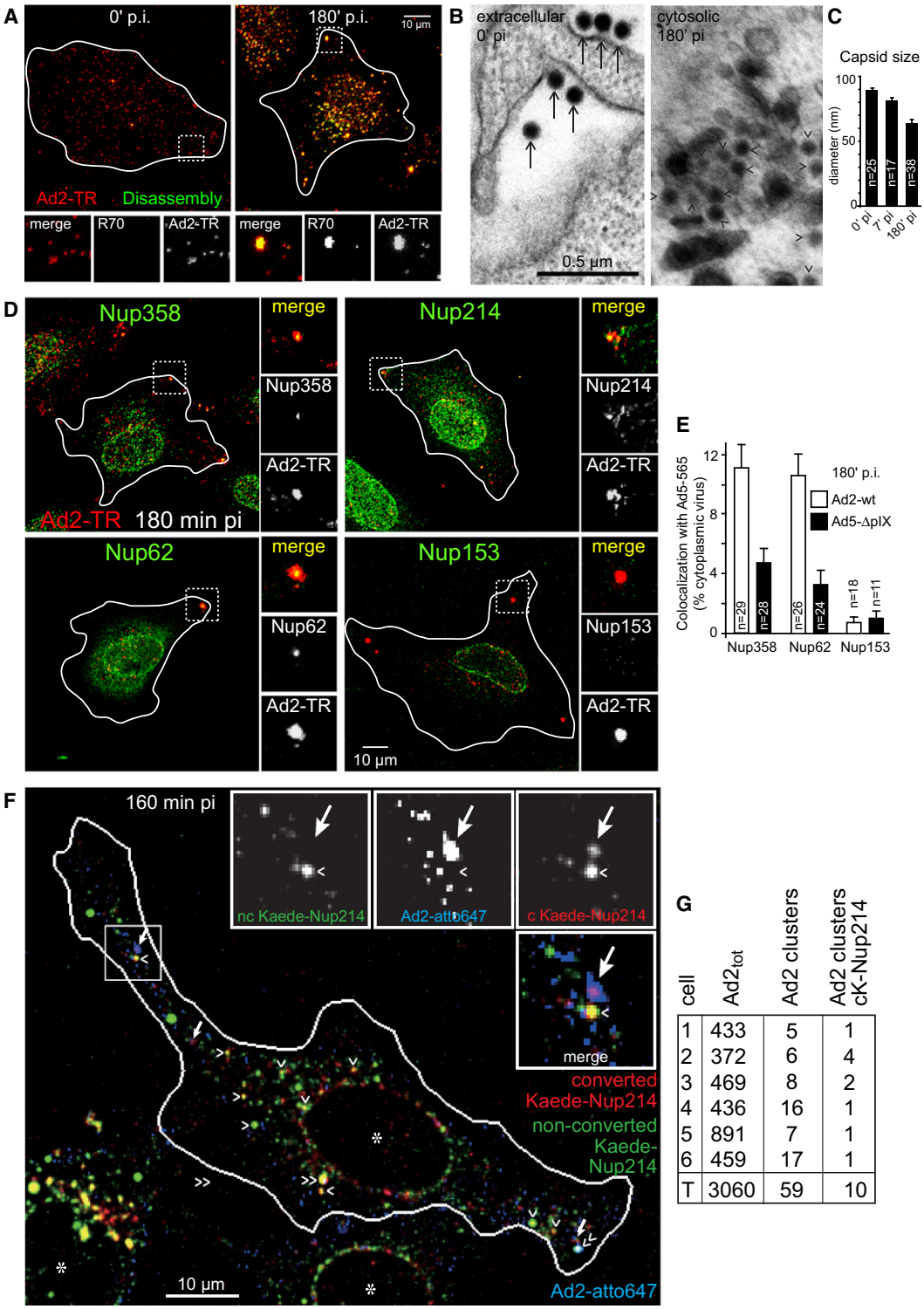

Figure 1. Nucleoporins Are Picked Up from the Nuclear Envelope by the Incoming Virus and Transported on Disassembled Capsids to the Periphery

(A) Clusters of disassembled Ad2-TR stained by the conformation sensitive anti-hexon antibody R70 in the cytoplasm and cell periphery 180 min p.i. See also Figure S1A.

(B) Disassembled cytosolic capsids (arrowheads) are smaller than extracellular viruses (arrows) analyzed by EM at 0 min (cold-bound viruses) or 180 min p.i. See also Figure S1A.

(C) Mean values of capsid diameters including SEM and number of capsids (n) analyzed from two independent experiments.

Mandelkow, 2002), while the C terminus contains six tetratricopeptide repeats (TPRs) of about 34 amino acids and is involved in cargo binding interactions (Hirokawa et al., 2009). We used GFP fused to the TPR domain of Klc2 (which is very similar to that of Klc1) and could confirm that viruses recruited kinesin-1 via the light chain (Figure 2C). The colocalization of Ad2-TR with GFP-TPR not only increased from 0 to 30 min p.i. coincident with the arrival of particles in the cytosol and the very first particles at the nucleus, but more interestingly, after 60 min p.i. when most particles had reached the nucleus, and disassembly measurably commenced, GFP-TPR was increasingly found on R70-positive structures (Figure 2D; Trotman et al., 2001). The overexpression of GFP-TPR, however, reduced the appearance of R70-positive capsids, and lowered infection by about 50%, suggesting that it worked as a dominant negative for kinesin-1 function (Figures 2E and 2F), as shown previously for vaccinia virus (Rietdorf et al., 2001). The reduction in the level of infection was not due to a lack of targeting to the nuclear envelope or entry of viruses into the cytosol, as demonstrated by confocal fluorescence microscopy and TEM analysis (Figure S2A). In contrast to GFP-TPR, overexpression of GFP-tagged p50 dynamitin inhibited targeting of Ad2 to the nuclear envelope and infection (Figure S2A), consistent with the established role of dynein/dynactin complex in Ad2 transport to the nucleus (Bremner et al., 2009; Engelke et al., 2011; Suomalainen et al., 1999). These inhibition results, together with the finding that there were only low levels of TPR-GFP on incoming Ad2-TR before disassembly (Figure 2D), suggest that GFP-TPR inhibited infection after virus attachment to the NPC due to blocking of kinesin-1 recruitment.

Given this result, we tested the involvement of kinesin-1 in Ad2/5 infection by using small interfering RNAs (siRNAs) against kinesin light-chain Klc1 and heavy-chains Kif5B and Kif5C. RNA interference against Klc2 had no effect (data not shown). Kif5B and Kif5C are expressed in a variety of tissues and involved in morphogenetic processes and anterograde transport of mitochondria and vesicles in neuronal cells, although the function of Kif5C in epithelial cells is not known (reviewed in Astanina and Jacob, 2010). siRNA against Klc1 and Kif5C but not Kif5B reduced Ad2 infection and capsid uncoating (Figures 2G–2I). All the siRNAs reduced the corresponding mRNAs as determined by quantitative PCR, and did not affect the delivery of Ad2 particles to the cytosol (Figure S2B, data not shown). These observations suggest that Klc1/2 and Kif5C are associated with Ad2 particles, particularly disassembled capsids in the cytoplasm, and are required for infectious capsid disassembly at the nuclear envelope.

Kinesin Light Chain Binds Protein IX of Intact and Disrupted Particles

To address how kinesin-1 is recruited to the viruses, we incubated triple CsCl-purified intact or heat-disrupted Ad2 particles with GST-TPR or GST alone (Figure 3A, top two panels). Ad2 particles were disassembled by heat disruption, which opens up the capsids and releases internal pV (Puntener et al., 2011). Western blot analysis against hexon revealed that GST-TPR immobilized on glutathione Sepharose beads or GST-Klc2 (data not shown), but not GST pull-down Ad2 particles or hexon from heat-disrupted particles (Figure 3A, third panel from top). Heat disruption gave rise to capsomers, including the group of nine hexons stabilized by pIX (Figure 3B, inset; Liu et al., 2010). Similarly, biotinylated Ad2 on streptavidin-coated beads bound GST-TPR but not GST (Figure 3C).

To determine which viral protein is responsible for recruiting kinesin-1, we analyzed the profile of [^{35}S]-methionine viral proteins from heat-denatured Ad2 that were capable of binding GST-TPR. GST-TPR pulled down major fractions of hexon (II), the capsid-stabilizing proteins IIIa and IX, and small amounts of fiber (IV) (Figure 3A, lowest panel, asterisks). Control pull-downs with intact Ad2 yielded the complete spectrum of virion proteins (Figure 3A, lowest panel). We focused our attention on pIX, since pIIIa and fiber are shed from the incoming virions at the plasma membrane and endosomes (Greber et al., 1993). pIX is conserved in mammal-tropic mastadenoviruses (Davison et al., 2003). Moreover, the localization of pIX on the virus is consistent with a potential interaction with Klc1/2, as its N terminus and the central domain tightly adhere to the outside of the virion, and the C terminus projects away from the surface of the virus (Liu et al., 2010).

Immunoprecipitation of myc-tagged pIX from lysates of transfected cells confirmed that pIX interacts with HA-tagged Klc1 (Figure 3D). An interaction between the two proteins was further supported by the observation that Ad5-ΔpIX (mutant strain dl313) or purified hexon bound ~20 times less to GST-TPR than wild-type Ad5 as determined by densitometric scanning (Figure 3E). The sequence of pIX of Ad2 and Ad5 are 100% conserved except for amino acid residue three. This contrasts the major antigenic determinants, hexon and fiber, which have 87% and 69% identities between Ad2 and Ad5 serotypes, respectively. The almost 100% sequence conservation of pIX suggests that the protein plays an important but undefined role during virus infection. Given this, we examined whether pIX has a role in infection, as measured by accumulation of newly synthesized viral antigens in the nucleus. Infection of HeLa cells with

(D) Displacement of Nup358, Nup214, and Nup62 to the cytoplasm in the presence of 0.1 mg/ml cycloheximide 180 min p.i. Fixed cells were analyzed by single-section CLSM with cell borders outlined from DIC images. See also Figures S1B and S1C and Movie S1.
(E) Quantification of immunostained Nup358, Nup62, and Nup153 colocalizing with cytoplasmic Ad5-atto565 and Ad5ΔpIX-atto565, respectively, normalized for atto565 signal. n, number of analyzed cells from two independent experiments. Error bars indicate SEM.
(F) Localization of photoconverted Kaede-Nup214 from the nuclear envelope area to cytoplasmic clusters of virus capsids 160 min p.i. A merged triple color image from confocal sections shows nonconverted Kaede-Nup214 (green), Ad2-atto647 (blue), and photoconverted Kaede-Nup214 (red) with corresponding single channels of a cytoplasmic area of interest (boxed), and the outline of the corresponding cell determined from the DIC image (white line, data not shown). The arrows indicate Ad2-atto647 clusters, which are positive for photoconverted and negative for nonconverted Kaede-Nup214. Arrowheads (in the main image) point to puncta of converted and nonconverted Kaede-Nup214 with subthreshold levels of Ad2-atto647. Double arrowheads point out a minority of Ad2-atto647 particles double positive for converted and nonconverted Kaede-Nup214. Asterisks (*) mark photoactivated nuclei from three different cells. See also Figure S1D.
(G) Quantification of fluorescence intensity ($Ad2_{tot}$) and number of Ad2 particles positive for photoconverted Kaede-Nup214 (cK-Nup214), including Ad2 clusters and total number of Ad2 particles in six different photoconverted cells expressing Kaede-Nup214.

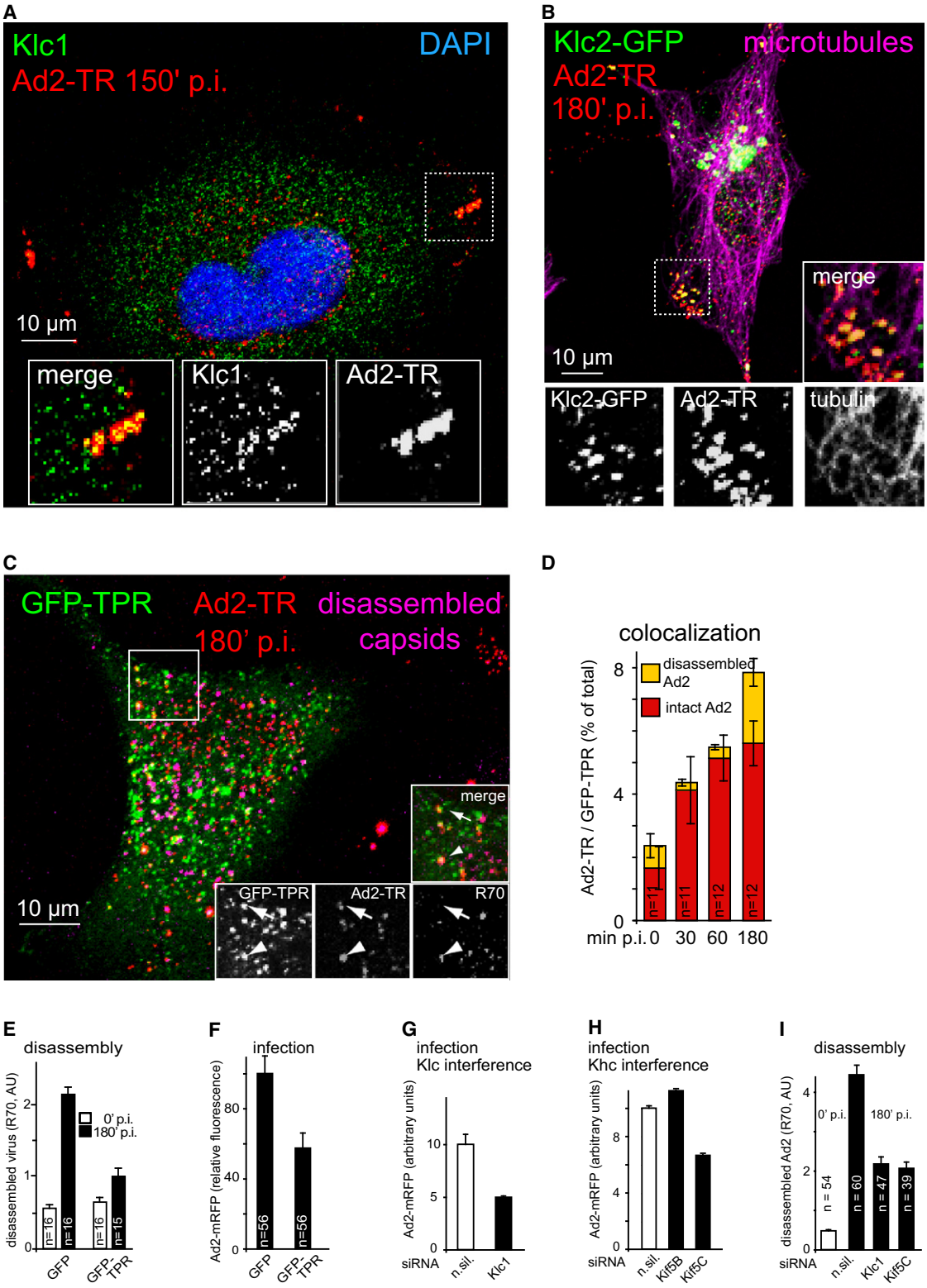

Figure 2. Kinesin-1 Supports Adenovirus Disassembly and Infection

(A) Immunofluorescence analysis of incoming Ad2-TR reveals colocalization with endogenous Klc1 in the cell periphery 150 min p.i. See also Figure S2A.

(B) Colocalization of Ad2-TR with transiently expressed Klc2-GFP in the cell periphery near microtubules 180 min p.i. See also Movie S2 and Figure S2A.

(C) Transiently expressed GFP-TPR colocalizes with disassembled Ad2-TR particles (arrowheads) visualized by R70 staining, unlike intact Ad2 (arrows) in the cell periphery 180 min p.i. See also Figure S2A.

Ad5-ΔpIX was significantly reduced compared to wild-type Ad5, although Ad5-ΔpIX particles localized to the nucleus with similar or even higher efficiency compared to Ad5 (Figures 3F and 3G).

Our observations are consistent with an earlier report showing that the reduced infectivity of Ad5-ΔpIX was independent of a putative transcriptional activity of pIX, and that Ad5-ΔpIX was impaired in viral propagation (Sargent et al., 2004). They do not necessarily contradict the observation that transgenic Ad5-ΔpIX expressed slightly more luciferase reporter from the strong cytomegalovirus (CMV) promotor than pIX-positive Ad5 (de Vrij et al., 2011). The CMV promotor is stimulated by kinases from the interferon response, and slow-growing viruses, such as Ad5-ΔpIX, elicit stronger interferon responses than fast-growing viruses (Schaack et al., 2011). Hence Ad5-ΔpIX is expected to have higher CMV-promotor activities than Ad5-containing pIX. Collectively, our data show that Klc1/2 binds to pIX and supports the uncoating of incoming viruses.

Kif5C Attachment to Nup358 Supports Infectious Virus Disassembly

Previous observations showed that Kif5C heavy chain interacts with the kinesin binding domain JX2 of Nup358 (Cho et al., 2007), which is anchored to Nup214 of the NPC (reviewed in D'Angelo and Hetzer, 2008), and extends approximately 150 nm from the nuclear membrane into the cytoplasm. We tested if attachment of Ad2 to the NPC was required for uncoating and infection. Knockdown of the adenovirus docking site Nup214 by RNA interference inhibited targeting of Ad2-atto565 to the nuclear envelope similarly to treatment with the microtubule-depolymerizing agent nocodazole, while knockdown of Nup358 had no effect, although the knockdown of Nup358 was stronger than Nup214 (Figure S3). In contrast, Nup214 or Nup358 knockdown inhibited the uncoating of Ad2-GFP-pV, as indicated by increased GFP-pV in the Ad2 capsids at 150 min p.i. compared to no or scrambled siRNA-treated cells (Figures 4A and 4B, and data not shown), and blocked the peripheral R70 signals (data not shown). These data indicate that adenovirus infection requires Nup214 and Nup358 for uncoating, but only Nup214 is involved in viral attachment to the NPC.

We next tested if Nup358 and kinesin-1 were functionally linked with each other. Using cryo-immunoelectron microscopy employing the Kif5C/5A-specific antibody H1 (which reacts with the major form of heavy chain of nonneuronal KHC near the N terminus), we found that Kif5C/5A was associated to Ad2-free NPCs, or NPCs containing docked Ad2 (Figure 5A). Quantification of immunogold from samples that were not treated with the H1 antibody indicated that the labeling for kinesin-1 was specific (Figure 5B). Since Kif5A does not bind to Nup358 (Cho et al., 2007), these data suggested that Kif5C localizes to the NPC independently of Ad2. The knockdown of Nup358 reduced Ad5-mediated GFP expression from 51.1% to 19.7% (Figures 5C and 5D). The ratios of GFP expression in transfected over nontransfected cells were 2.4 for empty plasmid control and 0.65 for the plasmid encoding Nup358-interfering RNA (quadrant 2 divided by quadrant 4), indicating a nearly 4-fold inhibition of infection by Nup358 interference. Expression of Nup358-interfering RNA inhibited the appearance of peripheral R70-positive capsids but did not affect the localization of incoming Ad2-TR at the nuclear envelope (Figures 5C and 5E). Importantly, Nup358 was not required for expression of GFP from herpes simplex virus but specifically for adenovirus, indicating that Nup358 depletion did not affect viral gene expression nonspecifically (Figure S4). This is consistent with the observation that HSV1 uses Nup214 rather than Nup358 for attachment to the NPC (Copeland et al., 2009; Pasdeloup et al., 2009). Further to the requirement of full-length Nup358, Ad2-mRFP transduction was inhibited by the expression of the JX2 domain of Nup358 fused to GFP (Figure 5F). JX2 binds to and activates kinesin-1 (Cho et al., 2009), suggesting that active kinesin-1 at Nup358 is required to enhance infection. This result was strengthened by the observation that Ad2-mRFP transduction was also inhibited by overexpressing a monomeric N-terminal motor domain construct of Kif5C (amino acids 1–332) that lacks the Nup358 binding domain (amino acids 827–923). Together, these data indicate that an interaction of Kif5C with the JX2 domain of Nup358 supports adenovirus infection but is not required for localization of the virus to the nuclear envelope.

The Displacement of Nups from the NPC Increases Infection and Nuclear Envelope Permeability

So far, the data indicated that the kinesin-1 motor protein binds to the viral capsid and the NPC, releases Nups from the nuclear envelope during capsid disruption, and thereby disperses capsid-Nup complexes to the cell periphery and promotes infection. To test if the loss of Nups from NPCs disrupted the integrity of the nuclear envelope, we microinjected inert fluorescent dextran molecules into the cytoplasm of HeLa cells, infected the cells for up to 180 min, and measured the steady-state distribution of dextran fluorescence in the nucleus and the cytoplasm by live-cell confocal fluorescence microscopy. While the gel filtration-purified 2000 kDa dextran-tetramethylrhodamine (TMR, fractions f27–32; see Figure 6D) remained excluded from the nucleus, 500 kDa dextran-fluorescein-isothiocyanate (FITC, f44–49, comprising dextrans that are slightly smaller than the peak of the 500 kDa dextran-FITC, see the Supplemental

(D) GFP-TPR colocalization with R70-positive particles increases with infection time (yellow bars), but GFP-TPR colocalization with R70-negative Ad2-TR remains constant 30 min p.i. (red bars). Representative mean values from several independent experiments including SEMs are shown. n, number of cells. See also Figure S2A.

(E) Inhibition of virus disassembly in GFP-TPR-expressing cells measured by R70 staining. Shown are mean values with SEM and number of cells (n).

(F) Inhibition of Ad2-mRFP infection by overexpression of GFP-TPR, analyzed by single-cell confocal microscopy 12 hr p.i. Shown are mean values with SEM and number of cells (n). See also Figure S2A.

(G and H) siRNA-mediated knockdown of Klc1 or Kif5C reduces Ad2-mRFP expression compared to nonsilencing (n.sil.) or Kif5B siRNAs, measured by flow cytometry 12 hr p.i. Mean values from three independent experiments are shown, with 10,000 cells counted in each experiment and error bars indicating SEM. For details, see also Figure S2B.

(I) Knockdown of Klc1 or Kif5C reduces Ad2 disassembly measured by R70 staining. Shown are mean values with SEM. See also Figure S2B.

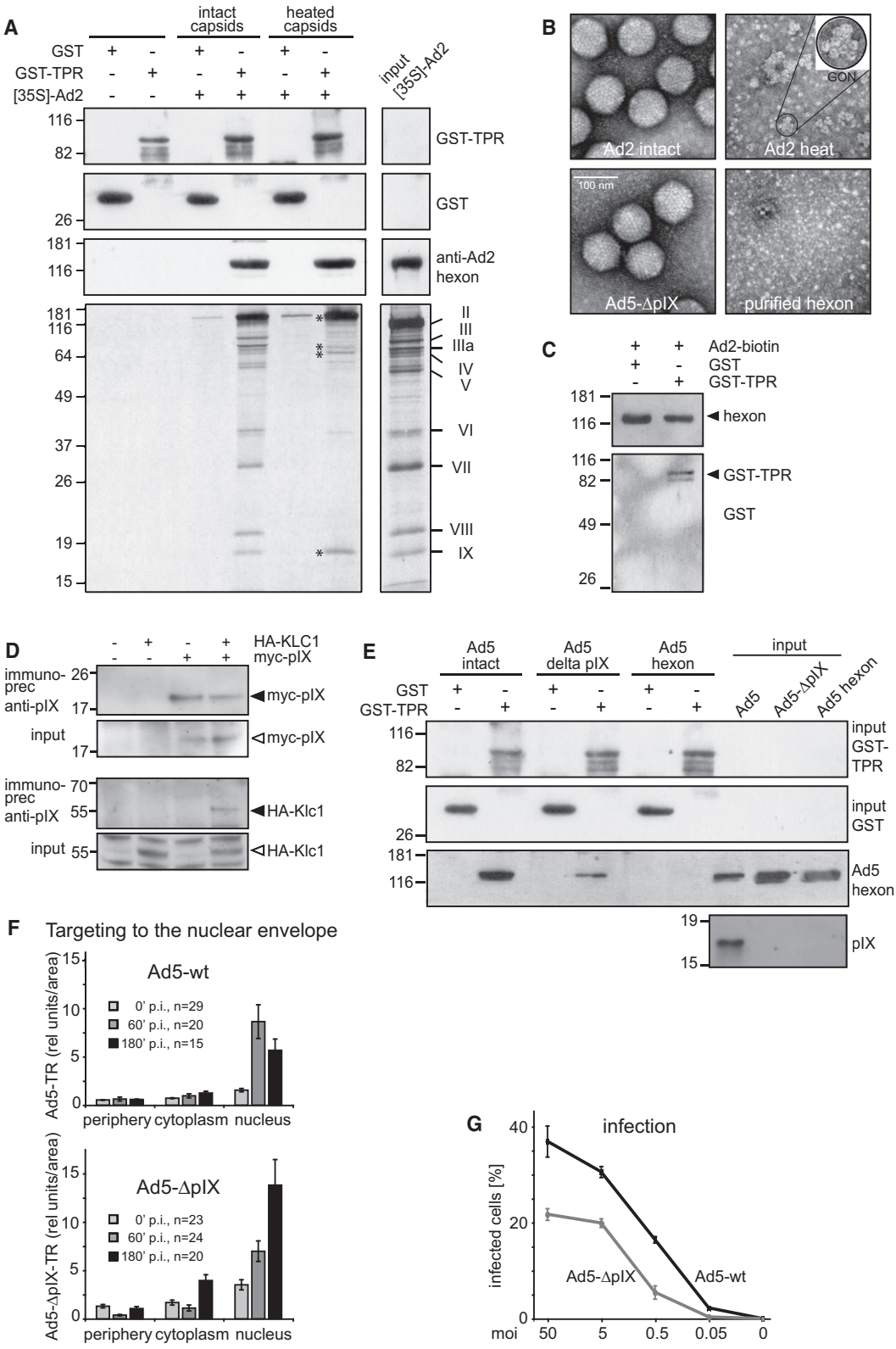

Figure 3. Ad2 Binds the TPR Domain of Klc1/2 through the Capsid Protein pIX

(A) Intact or heat-disrupted [^{35}S]-methionine-labeled Ad2 particles were incubated with recombinant GST-TPR or GST on glutathione Sepharose, washed, and analyzed by western blotting against GST (top two rows), against hexon (third row) or by autoradiography (fourth row). Note that GST-TPR bound similar amounts

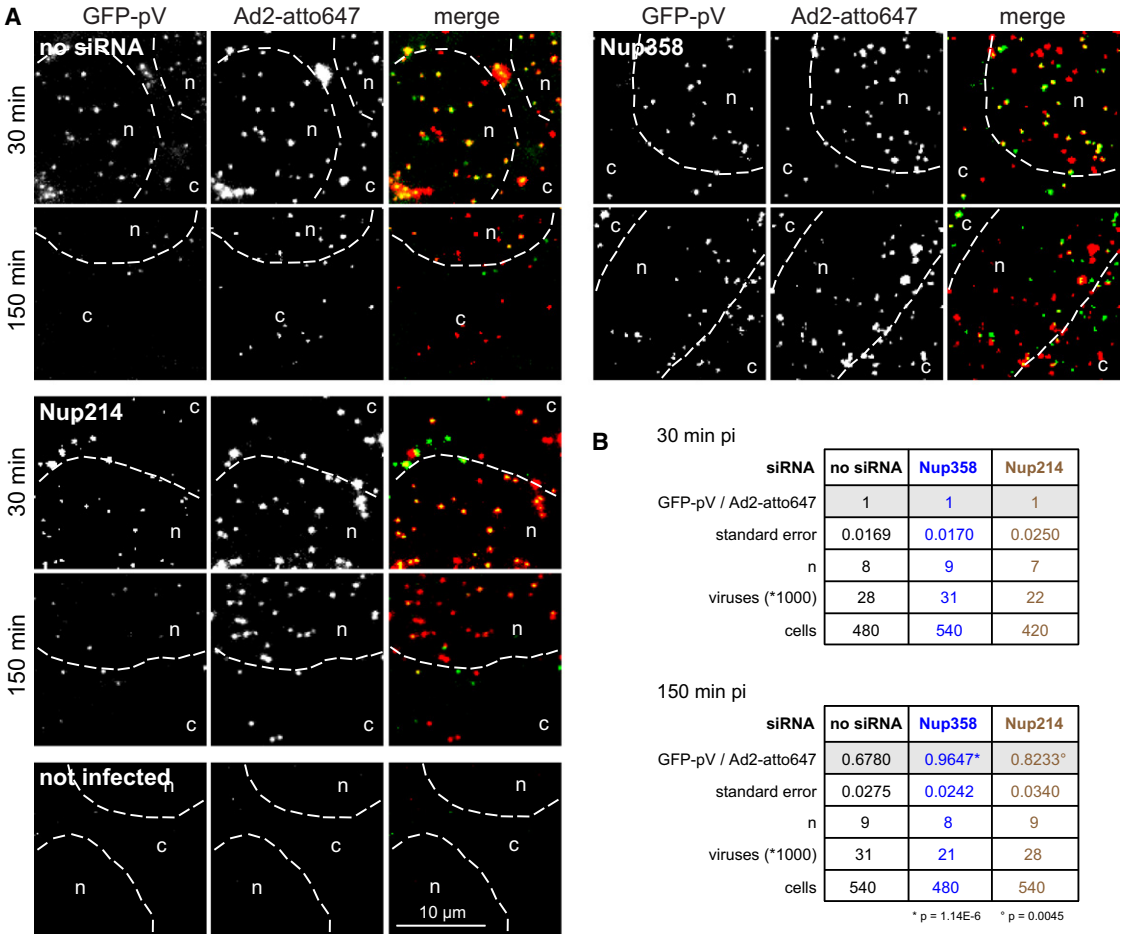

B

30 min pi

siRNA	no siRNA	Nup358	Nup214
GFP-pV / Ad2-atto647	1	1	1
standard error	0.0169	0.0170	0.0250
n	8	9	7
viruses (*1000)	28	31	22
cells	480	540	420

150 min pi

siRNA	no siRNA	Nup358	Nup214
GFP-pV / Ad2-atto647	0.6780	0.9647*	0.8233°
standard error	0.0275	0.0242	0.0340
n	9	8	9
viruses (*1000)	31	21	28
cells	540	480	540

* p = 1.14E-6 ° p = 0.0045

Figure 4. Nup358 or Nup214 Is Required for the Release of GFP-pV from Adenovirus

(A) Human embryonic retinoblast 911 cells were treated with siRNAs against Nup358 or Nup214 and infected with atto647-labeled Ad2-GFP-pV for 30 min or 150 min, fixed, and analyzed for capsid (atto647) and GFP fluorescence. Ad2-GFP-pV virions contain about 38 GFP-pV molecules, of which about two-thirds are released within the first 30 min during virus entry, and one-third at the NPC (Puntener et al., 2011). n denotes nucleus and c cytoplasm.

(B) Table with the mean of GFP-pV fluorescence per Ad2-atto647, including number of viruses, cells, experiments (n), standard errors, and p values compared to no siRNA-treated cells. See also Figure S3.

Information) and the broad-range 40 kDa dextran-FITC (eluting in fractions 35–64) were found in the nucleus of infected but not uninfected cells (Figures 6A–6E). The 40 kDa dextran-FITC is near the diffusion barrier of the NPC, whereas larger dextrans enter the nucleus only, when the NPCs are disrupted (Lenart and Ellenberg, 2006; Mohr et al., 2009). Our results therefore suggest that the NPCs of adenovirus-infected cells are partly disrupted. Interestingly, this disruption was transient, since cells

of hexon and pIX from both intact and heat-disrupted virions but less penton base (III), fiber (IV), and inner capsid proteins (V, VI, VII, VIII) from heat-ruptured than intact virions.

(B) Transmission electron micrographs of purified viruses stained with uranyl acetate reveal groups of nine hexons (GONs, inset) of heat-disrupted Ad2 but not purified hexon, which is free of pIX (data not shown).

(C) Binding of biotinylated Ad2 to GST-TPR-glutathione Sepharose measured by western blotting against GST and hexon.

(D) Coimmunoprecipitation of HA-tagged Klc1 with myc-tagged pIX. HEK293T cells were transfected with the indicated constructs, cell lysates immunoprecipitated with anti-pIX antibodies, and immuncomplexes blotted with anti-myc (upper panel) and anti-KLC antibodies (lower panel). Input panels are shown below the blots.

(E) Ad5 and much less Ad5-ΔpIX (dl313) capsids or HPLC-purified hexon protein bind to GST-TPR as indicated by GST pull-down experiments and western blotting against hexon and pIX. Relative molecular weights are indicated in kDa.

(F) Analyses of subcellular localization of fluorescent Ad5 and Ad5-ΔpIX (dl313) indicate that pIX is not required for cytoplasmic transport of the virus to the nuclear envelope. The y axis plots the fluorescence of viruses normalized per unit area. n, number of cells analyzed; error bars, SEM values.

(G) pIX is required for efficient Ad5-mediated gene expression. Human embryonic retinoblast 911 cells were infected with different amounts of Ad5-wt and Ad5-ΔpIX (dl313) and analyzed for penton base and fiber expression by confocal microscopy 15 hr p.i. (mean values of triplicates, with SEMs; moi, multiplicity of infection upon cold synchronization).

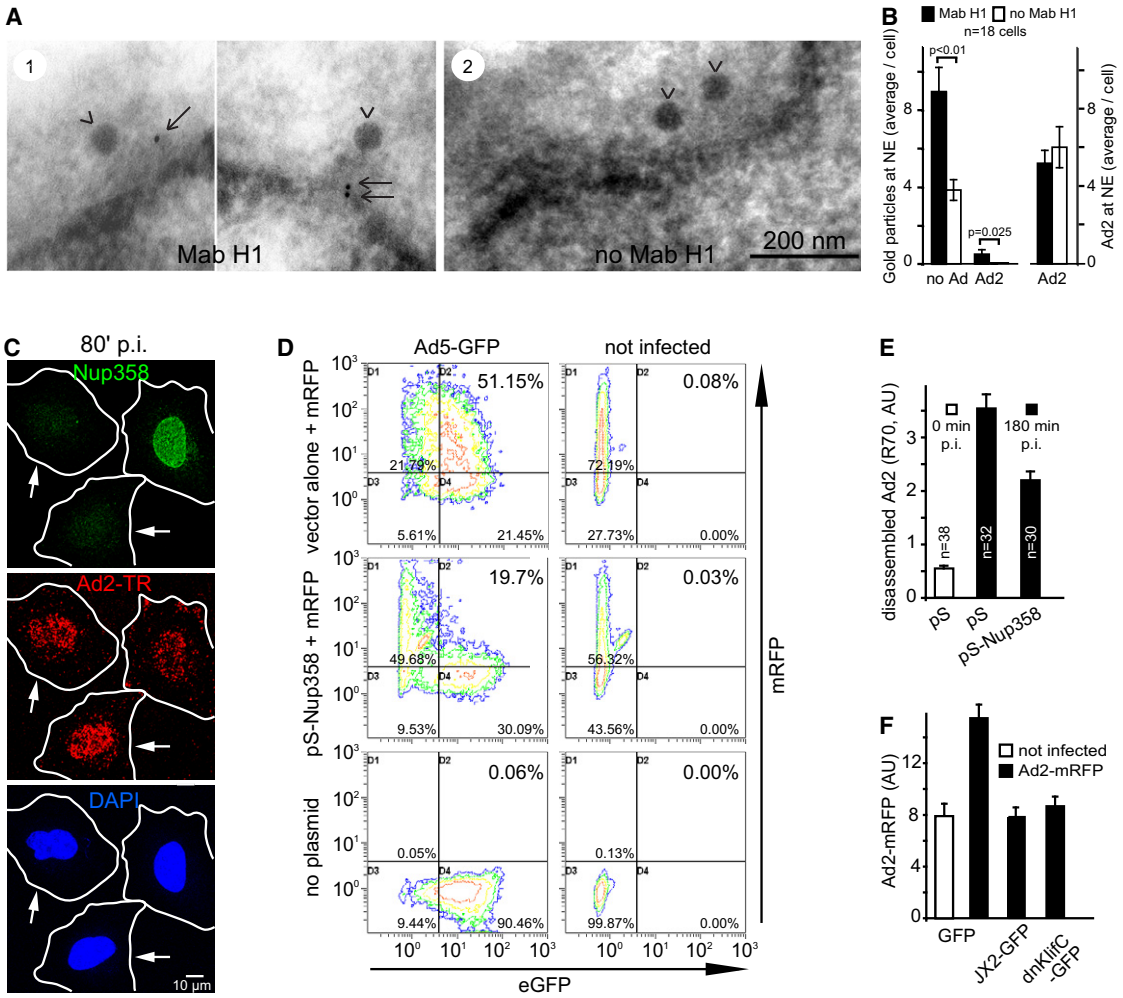

Figure 5. NPC-Localized Kif5C Supports Viral Disassembly

(A) Kif5C localizes to NPC-docked Ad2. HeLa cells infected with Ad2 for 60 min were processed for cryo-immunoelectron microscopy using the Kif5A/C-specific mouse monoclonal antibody Mab H1. Immunogold-labeled Kif5C (arrows) was found at Ad2-docked NPCs (arrow heads) less than 200 nm away from the virions and the nuclear membrane (panel 1). Little gold particles were detected in samples incubated without Mab H1 (panel 2).

(B) Left side depicts the quantification of Kif5A/C gold particles at the nuclear envelope (NE) in uninfected cells (no Ad), or at the nuclear envelope of infected cells in close proximity to Ad2 particles (<200 nm) (Ad2). The numbers of Ad2 particles at the nuclear envelope (normalized per cells, including SEM and number of cells analyzed = 18 for infected and uninfected cells) with or without Mab H1 staining is shown as a pair of columns on the right side. P values were derived from Student's t tests.

(C) Knockdown of Nup358 does not reduce transport of Ad2-TR to the nucleus. Cells transfected with pS-Nup358 for 84 hr were infected with Ad2-TR for 80 min, fixed, and processed for immunofluorescence staining using anti-Nup358 antibodies. Nup358 knockdown cells are pointed out by arrows. Note the reduced amounts of Ad2-TR in the periphery of Nup358 knockdown cells. Total intensity projections of confocal stacks including DAPI stainings are shown. See also Figure S4.

(D) Knockdown of Nup358 reduces the transduction of Ad5-GFP. HeLa cells were cotransfected with pS-Nup358 and mRFP-encoding plasmids, infected with Ad5-GFP, fixed at 6 hr p.i., and analyzed by flow cytometry. The upper right quadrant shows transfected cells (mRFP-positive) that are infected (GFP-positive).

(E) pS-Nup358-mediated knockdown of Nup358 inhibits Ad2 capsid disassembly compared to empty vector pS (pSuper), measured with the disassembly-specific anti-hexon antibody R70. Graphs represent mean values of analyzed cells (n).

(F) Expression of the kinesin heavy-chain binding domain JX2-GFP derived from Nup358, or dominant-negative (dn) Kif5C-GFP, reduces Ad2-mediated mRFP expression 12 hr p.i. Graphs represent mean values of analyzed cells, including SEM. Cells analyzed were 10, 50, 43, and 62 for the four conditions from left to right.

infected for 240 min prior to injection of the broad-range 40 kDa dextran-FITC excluded the dextran from the nucleus even stronger than did noninfected cells (Figure 6E).

To test if virus docking to the NPC was required to trigger nuclear leakage, we treated cells with the nuclear export inhibitor LMB, which blocks virus docking to the NPC (Strunze et al., 2005). LMB inhibited the influx of the broad-range 40 kDa dextran, although it did not block it completely (Figure 6E). These results were confirmed in cells treated with siRNAs against the adenovirus docking receptor Nup214 or the kinesin receptor Nup358, both of which strongly inhibited virus-induced nuclear leakage of 40 kDa dextran-FITC (Figure 6F). The knockdown of neither Nup214 nor Nup358 induced significant nuclear leakage by itself, implying that multiple Nups may be displaced by

adenovirus to allow dextran influx. We also tested if the kinesin light-chain binding protein pIX was involved in nuclear envelope disruption. Infection with Ad5ΔpIX, which did not recruit Nup358 and was not clustered in the cell periphery (Figure 1E and Figure S1B), did not significantly increase the nucleocytoplasmic ratio of 40 kDa dextran-FITC. The results indicate that pIX is important not only for capsid disassembly but also for increasing the permeability of the nuclear envelope during virus entry (Figure 6G).

DISCUSSION

How viruses transport and activate their genome in the nucleus has been a long-standing question in infectious disease biology. Genome activation invariably requires uncoating from a protecting protein shell, which, however, triggers potent innate immune responses against the exposed viral nucleic acids (reviewed in Wilkins and Gale, 2010).

Here we found a microtubule motor-based mechanism for uncoating of adenoviral DNA, for disrupting the NPCs and facilitating nuclear import of viral DNA (Figure 7). Adenoviruses undergo a stepwise uncoating program, which culminates with DNA release into the nucleus (Greber et al., 1993). Since we see very little colocalization of kinesin-1 with incoming viruses and interference with kinesin-1 or the kinesin-1 binding partner of the virus pIX has no negative effects on targeting the virus to the nuclear envelope, we suggest that subviral capsids recruit kinesin-1 at the NPC. At the NPC docking site Nup214, the subviral capsid is largely composed of the major capsid protein hexon and viral DNA. The hexon facettes are stabilized by multiple copies of pIX and the viral DNA condensed by proteins pVII, pV, and pX (Puntener et al., 2011). The particle becomes subject to a pulling force from the Kif5C heavy chain. Kif5C is activated by its binding partner Nup358 (Cho et al., 2009) and tethered to the particle by Klc1, which binds pIX. The particle thereby acts as a cooperative scaffolder and engages multiple kinesin-1 motors, which could move on NPC-proximal microtubules (Joseph and Dasso, 2008). This explains an earlier observation, namely, why nocodazole-induced loss of microtubules inhibited infection both during cytoplasmic transport and thereafter (Mabit et al., 2002). Particle disruption presumably results in the release of group of nine hexon trimers (GONs), still stabilized by pIX (Liu et al., 2010; Reddy et al., 2010). Some of the GONs may remain bound to Nup214 and continue to be subject to pulling forces by kinesin-1. Hexon binding to Nup214 may weaken the anchoring of Nup214 in the NPC and thereby help to disrupt parts of the cytoplasmic structure of the NPC.

The work here shows how viral nucleic acids can be unlocked from the capsid for delivery into the nucleus through the NPC. The NPC is a selective gateway for proteins, nucleic acids, and solutes in and out of the nucleus. The FG-repeat barrier works by hydrophobic exclusion, and is particularly effective for very large molecules. Remarkably, the action of kinesin-1 at the NPC-docked virus disrupts the integrity of the NPC. This observation is similar but mechanistically distinct from a report showing an increase of nuclear envelope permeability from aged nuclei as a consequence of oxidation and proteolytic removal of Nup93 (D'Angelo et al., 2009). In both instances, viral infection and aged nuclei, signal-mediated nuclear import is not impaired (D'Angelo et al., 2009; Trotman et al., 2001). This is consistent with genetic deletion studies of FG and GLFG repeats of yeast Nups, which showed that NPC functionality is maintained in the absence of up to half of the FG-repeat mass (Strawn et al., 2004). It is also reminiscent of mitotic *Aspergillus nidulans* cells, where most of the NPC-peripheral Nups are dispersed to the cytoplasm, which leaves behind a minimal functional NPC (Osmani et al., 2006).

We have directly measured the disruption of the NPC integrity by the displacement of both central and peripheral Nups, which comprise cohesive and noncohesive Nups to stabilize the NPC (Alber et al., 2007; Galy et al., 2003). Interestingly, the displacement of FG-containing Nups increased the nuclear envelope permeability for hydrophilic dextran molecules. This is in agreement with studies in yeast, where genetic deletions of individual FG domains relaxed the NPC permeability barrier (Patel et al., 2007). Recent diffusion measurements of solutes have further suggested that the transit of relatively hydropobic receptor-cargo complexes and solutes occurs at least in part through the same channels built up by FG-repeat proteins (Mohr et al., 2009). The displacement of FG-containing Nups by adenovirus could hence enhance the import of the viral DNA genome through the diffusion channels. This is supported by the transient nature of the relaxed diffusion barrier, which argues that the viral DNA-protein complex competes with solutes for passage through the NPC.

Adenovirus DNA import also takes advantage of carrier-mediated transport mechanisms. The viral genome is a linear DNA of about 36 kbp, condensed into 140–180 nucleosome-like structures by the dimeric protein VII, the minor protein X, and the accessory protein pV (Chatterjee et al., 1985; Chen et al., 2007; Corden et al., 1976; Puntener et al., 2011; van Oostrum and Burnett, 1985). Since pVII but not pV remains associated with the DNA until import is completed (Puntener et al., 2011; Xue et al., 2005), several hundred import receptors are thought to cover the highly charged DNA-protein complex. Opening up of the diffusion channels prior to or during nuclear import could make DNA import less dependent on nuclear import factors. Importins beta1, beta2, and beta7 are known to be limiting for adenovirus infection, as suggested by antibody microinjection studies or cell free import assays (Hindley et al., 2007; Trotman et al., 2001), and mediate the import of the viral core-associated protein VII (Wodrich et al., 2006).

Collectively, by showing that kinesin-1 can disrupt both viral capsids and the NPC, we extend the known function(s) of kinesin motors, namely to get cargo into the nucleus. Our findings specifically show how kinesin-1 and Nup358 support viral uncoating at the NPC. This could be of interest also for other viruses, such as HIV, where Gag associates with Kif4, a member of the N-terminal kinesin superfamily (Tang et al., 1999), and Nup358 and Nup153 have potential roles for provirus formation in the nucleus (Brass et al., 2008).

EXPERIMENTAL PROCEDURES

Antibodies, Chemicals

Rabbit antibodies against hexon R70, fiber R72, and penton R73 were used as described (Trotman et al., 2001). Rabbit anti-pIX antibodies were from

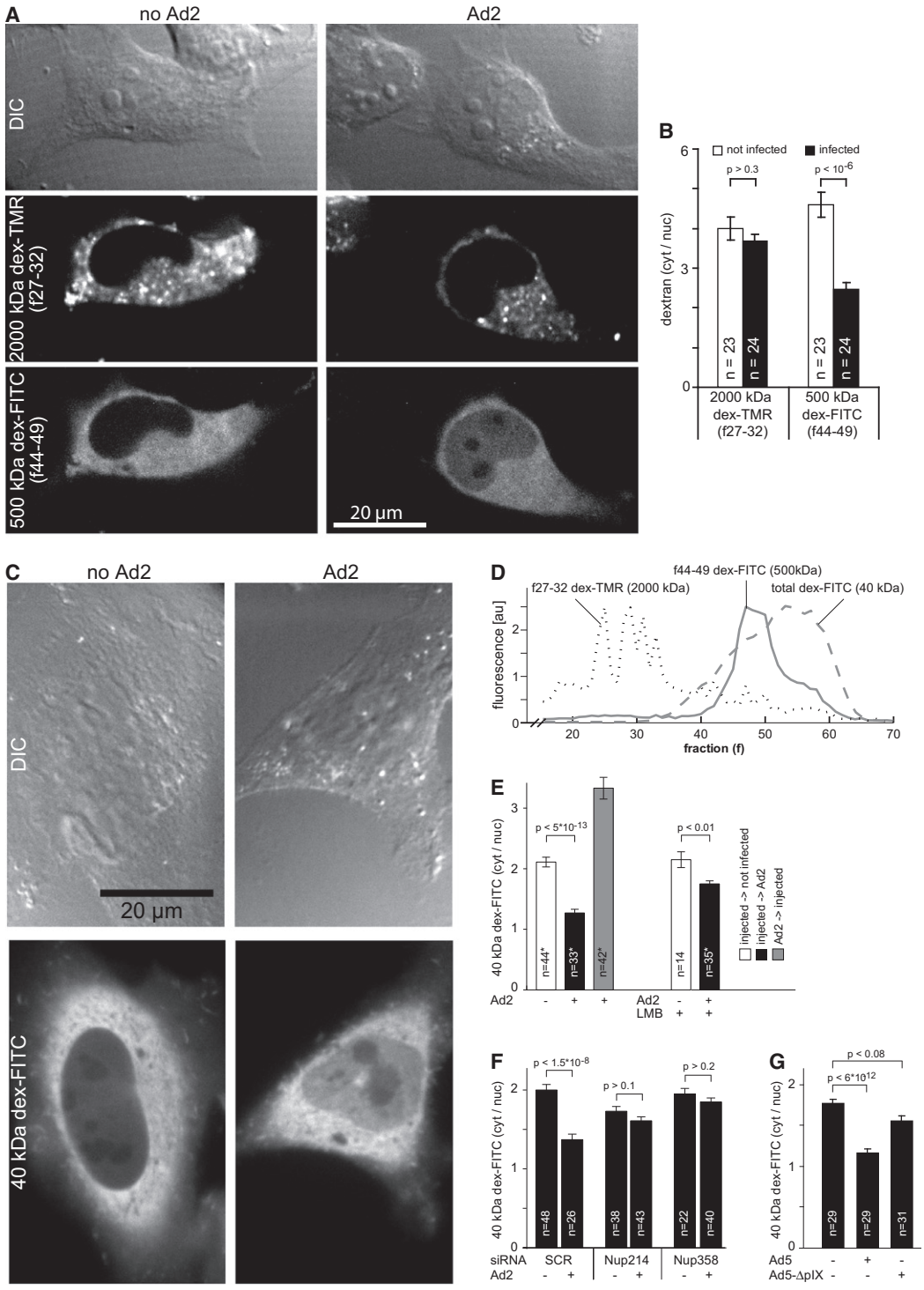

Figure 6. Adenovirus-Mediated Disruption of the NPC Leads to Dextran Influx into the Nucleus

(A and B) HeLa cells microinjected with a mixture of gel filtration-fractionated large-sized dextran-TMR (f27–32) and medium sized dextran-FITC (f44–49) were inoculated with Ad2 for 180 min, imaged by live-cell spinning disc confocal fluorescence microscopy, and analyzed for nuclear and cytoplasmic dextran.

(C) Cells microinjected with broad-range 40 kDa dextran-FITC were infected and imaged as described for (A).

(D) Analytical gel filtration profiles of injected 500 kDa dextran-FITC and 2000 kDa dextran-TMR, fractionated by Superose 6-HR 10/30 column, as well as broad-range (nonfractionated) 40 kDa dextran-FITC.

(E) HeLa cells injected with broad-range 40 kDa dextran-FITC were either treated or not with 20 nM leptomycin B (LMB), infected, and imaged as outlined in (A). Mean values of cytoplasmic to nuclear ratios are shown for infected cells (Ad2, black bars) or noninfected cells (open bars). Cells were also first infected with Ad2 for 240 min and then injected with 40 kDa dextran-FITC (gray bar).

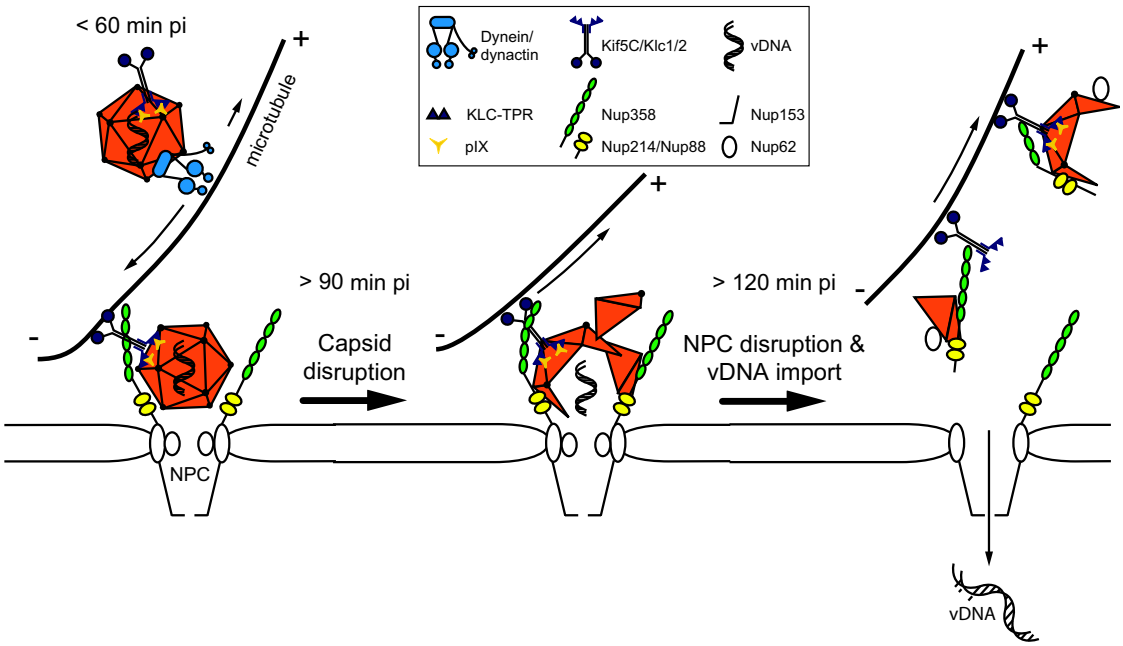

Figure 7. Model for Kinesin-1-Mediated Virus Disassembly at the NPC

Incoming adenovirus (red) traffics toward the nucleus using the microtubule minus end-directed motor complex dynein/dynactin, and attaches to the NPC by hexon interactions with Nup214. Viral capsids bind to the kinesin-1 light-chain Klc1/2 by the hexon-associated pIX. Nup358 attached to the Nup214/Nup88 complex (reviewed in D'Angelo and Hetzer, 2008) associates with kinesin-1 heavy-chain Kif5C via the JX2 domain, and possibly with microtubules through a distal microtubule-binding domain. Kinesin-1 motors disrupt the viral capsid, and dislocate Nup358/Nup214 and Nup62 from the central NPC channel to the periphery. The disruption of the NPC facilitates entry of the viral DNA into the nucleus.

M. Rosa-Calatrava (Rosa-Calatrava et al., 2001), and mouse L1 against Klc (Mab1613) and H1 against kinesin heavy chain (Khc) (Mab1616) were from Chemicon International (Pfister et al., 1989). H1 recognizes recombinant Kif5A and Kif5C but not Kif5B (Cai et al., 2001). Antibodies against the C terminus of Nup214 and Crm1 were from M. Fornerod (Fornerod et al., 1997), against Nup358 from F. Melchior (Hutten et al., 2008), and Mab SA1 against the carboxyl terminus of Nup153 from B. Burke (Bodoor et al., 1999).

Photoconversion of Kaede-Nup214

DNA encoding the photoconvertible fluorescent protein Kaede (pKaede-S1, MBL International Corporation, Woburn, MA, USA; Ando et al., 2002) was cloned into the expression vector containing human Nup214 cDNA (kindly provided by M. Fornerod) and transfected into HeLa-K cells with JetPEI (Polyplus Transfection, Illkirch, France) on 12 mm glass coverslips for 48 hr. Cells were mounted onto a homemade slide holder, overlaid with 0.5 ml live imaging medium (Hank's buffered salt solution with 0.5% BSA and 1 mg/ml ascorbic acid [pH 7.2–7.4]), inoculated with 0.5 μg of Ad2-atto647, and photoconverted in five optical layers across the entire nucleus with a UV laser at 355 nm in combination with a diode laser at 405 nm for 10 s on an SP5 Leica confocal laser scanning microscope recording the X-Y position of the photoconverted cells. Infection continued until 90–160 min, and entire optical stacks from photoconverted cells were acquired at 488, 561, and 633 nm excitation to record nonconverted Kaede-Nup214 and converted Kaede-Nup214 and Ad2-atto647. Single sections were analyzed for colocalization of converted Kaede-Nup214 and Ad2-atto647, and images were displayed after deconvolution by Huygens software (Scientific Volume Imaging, Hilversum, The Netherlands). The total number of Ad2-atto647 particles was analyzed by maximum projections of image stacks and processing by a global threshold method.

Other Procedures

Cells, viruses, cDNAs, transfections, recombinant proteins, pull-downs, coimmunoprecipitation, infections, image acquisitions and analyses, and purification and microinjection of dextrans are described in the Supplemental Information.

SUPPLEMENTAL INFORMATION

Supplemental Information includes four figures, two movies, Supplemental Experimental Procedures, and Supplemental References and can be found with this article online at doi:10.1016/j.chom.2011.08.010.

ACKNOWLEDGMENTS

We thank Drs. Brian Burke, Maarten Fornerod, Silvio Hemmi, Rob Hoeben, Ulrike Kutay, Frauke Melchior, Kevin Pfister, Cornel Fraefel, and Manuel Rosa-Calatrava for reagents or virus stocks; and Maarit Suomalainen and Corinne Wilhelm for help with dextran purification and western blotting. This work was supported by the Swiss National Science Foundation (U.F.G.), the Kanton Zürich (U.F.G.), and Cancer Research UK (M.W.).

Received: October 1, 2009
Revised: March 23, 2011
Accepted: August 1, 2011
Published: September 14, 2011

(F) Mean values of cytoplasmic to nuclear ratios of cells treated with siRNA against Nup214, Nup358, or scrambled siRNA (SCR); microinjected with broad-range 40 kDa dextran-FITC; and infected or not infected.
(G) Ratios of cytoplasmic to nuclear dextran in cells microinjected with the broad-range 40 kDa dextran-FITC and infected with Ad5 or Ad5ΔpIX.
All graphs represent mean values of analyzed samples (n) including the SEM, and p values from Student's t tests.

REFERENCES

Alber, F., Dokudovskaya, S., Veenhoff, L.M., Zhang, W., Kipper, J., Devos, D., Suprapto, A., Karni-Schmidt, O., Williams, R., Chait, B.T., et al. (2007). The molecular architecture of the nuclear pore complex. Nature *450*, 695–701.

Ando, R., Hama, H., Yamamoto-Hino, M., Mizuno, H., and Miyawaki, A. (2002). An optical marker based on the UV-induced green-to-red photoconversion of a fluorescent protein. Proc. Natl. Acad. Sci. USA *99*, 12651–12656.

Astanina, K., and Jacob, R. (2010). KIF5C, a kinesin motor involved in apical trafficking of MDCK cells. Cell. Mol. Life Sci. *67*, 1331–1342.

Bernad, R., van der Velde, H., Fornerod, M., and Pickersgill, H. (2004). Nup358/RanBP2 attaches to the nuclear pore complex via association with Nup88 and Nup214/CAN and plays a supporting role in CRM1-mediated nuclear protein export. Mol. Cell. Biol. *24*, 2373–2384.

Bodoor, K., Shaikh, S., Salina, D., Raharjo, W.H., Bastos, R., Lohka, M., and Burke, B. (1999). Sequential recruitment of NPC proteins to the nuclear periphery at the end of mitosis. J. Cell Sci. *112*, 2253–2264.

Brass, A.L., Dykxhoorn, D.M., Benita, Y., Yan, N., Engelman, A., Xavier, R.J., Lieberman, J., and Elledge, S.J. (2008). Identification of host proteins required for HIV infection through a functional genomic screen. Science *319*, 921–926.

Bremner, K.H., Scherer, J., Yi, J., Vershinin, M., Gross, S.P., and Vallee, R.B. (2009). Adenovirus transport via direct interaction of cytoplasmic dynein with the viral capsid hexon subunit. Cell Host Microbe *6*, 523–535.

Burckhardt, C.J., Suomalainen, M., Schoenenberger, P., Boucke, K., Hemmi, S., and Greber, U.F. (2011). Drifting motions of the adenovirus receptor CAR and immobile integrins initiate virus uncoating and membrane lytic protein exposure. Cell Host Microbe *10*, 105–117.

Cai, Y., Singh, B.B., Aslanukov, A., Zhao, H., and Ferreira, P.A. (2001). The docking of kinesins, KIF5B and KIF5C, to Ran-binding protein 2 (RanBP2) is mediated via a novel RanBP2 domain. J. Biol. Chem. *276*, 41594–41602.

Chatterjee, P.K., Vayda, M.E., and Flint, S.J. (1985). Interactions among the three adenovirus core proteins. J. Virol. *55*, 379–386.

Chen, J., Morral, N., and Engel, D.A. (2007). Transcription releases protein VII from adenovirus chromatin. Virology *369*, 411–422.

Cho, K.I., Cai, Y., Yi, H., Yeh, A., Aslanukov, A., and Ferreira, P.A. (2007). Association of the kinesin-binding domain of RanBP2 to KIF5B and KIF5C determines mitochondria localization and function. Traffic *8*, 1722–1735.

Cho, K.I., Yi, H., Desai, R., Hand, A.R., Haas, A.L., and Ferreira, P.A. (2009). RANBP2 is an allosteric activator of the conventional kinesin-1 motor protein, KIF5B, in a minimal cell-free system. EMBO Rep. *10*, 480–486.

Copeland, A.M., Newcomb, W.W., and Brown, J.C. (2009). Herpes simplex virus replication: roles of viral proteins and nucleoporins in capsid-nucleus attachment. J. Virol. *83*, 1660–1668.

Corden, J., Engelking, H.M., and Pearson, G.D. (1976). Chromatin-like organization of the adenovirus chromosome. Proc. Natl. Acad. Sci. USA *73*, 401–404.

D'Angelo, M.A., and Hetzer, M.W. (2008). Structure, dynamics and function of nuclear pore complexes. Trends Cell Biol. *18*, 456–466.

Daigle, N., Beaudouin, J., Hartnell, L., Imreh, G., Hallberg, E., Lippincott-Schwartz, J., and Ellenberg, J. (2001). Nuclear pore complexes form immobile networks and have a very low turnover in live mammalian cells. J. Cell Biol. *154*, 71–84.

D'Angelo, M.A., Raices, M., Panowski, S.H., and Hetzer, M.W. (2009). Age-dependent deterioration of nuclear pore complexes causes a loss of nuclear integrity in postmitotic cells. Cell *136*, 284–295.

Davison, A.J., Benko, M., and Harrach, B. (2003). Genetic content and evolution of adenoviruses. J. Gen. Virol. *84*, 2895–2908.

de Vrij, J., van den Hengel, S.K., Uil, T.G., Koppers-Lalic, D., Dautzenberg, I.J., Stassen, O.M., Barcena, M., Yamamoto, M., de Ridder, C.M., Kraaij, R., et al. (2011). Enhanced transduction of CAR-negative cells by protein IX-gene deleted adenovirus 5 vectors. Virology *410*, 192–200.

Engelke, M.F., Burckhardt, C.J., Morf, M.K., and Greber, U.F. (2011). The dynactin complex enhances the speed of microtubule-dependent motions of adenovirus both towards and away from the nucleus. Viruses *3*, 233–253.

Fornerod, M., van Deursen, J., van Baal, S., Reynolds, A., Davis, D., Murti, K.G., Fransen, J., and Grosveld, G. (1997). The human homologue of yeast CRM1 is in a dynamic subcomplex with CAN/Nup214 and a novel nuclear pore component Nup88. EMBO J. *16*, 807–816.

Frey, S., and Gorlich, D. (2007). A saturated FG-repeat hydrogel can reproduce the permeability properties of nuclear pore complexes. Cell *130*, 512–523.

Galy, V., Mattaj, I.W., and Askjaer, P. (2003). Caenorhabditis elegans nucleoporins Nup93 and Nup205 determine the limit of nuclear pore complex size exclusion in vivo. Mol. Biol. Cell *14*, 5104–5115.

Gazzola, M., Burckhardt, C.J., Bayati, B., Engelke, M., Greber, U.F., and Koumoutsakos, P. (2009). A stochastic model for microtubule motors describes the in vivo cytoplasmic transport of human adenovirus. PLoS Comput. Biol. *5*, e1000623. 10.1371/journal.pcbi.1000623.

Greber, U.F., and Way, M. (2006). A super highway to virus infection. Cell *124*, 741–754.

Greber, U.F., Willetts, M., Webster, P., and Helenius, A. (1993). Stepwise dismantling of adenovirus 2 during entry into cells. Cell *75*, 477–486.

Greber, U.F., Suomalainen, M., Stidwill, R.P., Boucke, K., Ebersold, M., and Helenius, A. (1997). The role of the nuclear pore complex in adenovirus DNA entry. EMBO J. *16*, 5998–6007.

Hayashi, S., and Hogg, J.C. (2007). Adenovirus infections and lung disease. Curr. Opin. Pharmacol. *7*, 237–243.

Hindley, C.E., Lawrence, F.J., and Matthews, D.A. (2007). A role for transportin in the nuclear import of adenovirus core proteins and DNA. Traffic *8*, 1313–1322.

Hirokawa, N., Noda, Y., Tanaka, Y., and Niwa, S. (2009). Kinesin superfamily motor proteins and intracellular transport. Nat. Rev. Mol. Cell Biol. *10*, 682–696.

Hutten, S., and Kehlenbach, R.H. (2006). Nup214 is required for CRM1-dependent nuclear protein export in vivo. Mol. Cell. Biol. *26*, 6772–6785.

Hutten, S., Flotho, A., Melchior, F., and Kehlenbach, R.H. (2008). The Nup358-RanGAP complex is required for efficient Importin {alpha}/{beta}-dependent nuclear import. Mol. Biol. Cell *19*, 2300–2310.

Joseph, J., and Dasso, M. (2008). The nucleoporin Nup358 associates with and regulates interphase microtubules. FEBS Lett. *582*, 190–196.

Kojaoghlanian, T., Flomenberg, P., and Horwitz, M.S. (2003). The impact of adenovirus infection on the immunocompromised host. Rev. Med. Virol. *13*, 155–171.

Lee, K., Ambrose, Z., Martin, T.D., Oztop, I., Mulky, A., Julias, J.G., Vandegraaff, N., Baumann, J.G., Wang, R., Yuen, W., et al. (2010). Flexible use of nuclear import pathways by HIV-1. Cell Host Microbe *7*, 221–233.

Lenart, P., and Ellenberg, J. (2006). Monitoring the permeability of the nuclear envelope during the cell cycle. Methods *38*, 17–24.

Lim, R.Y., Fahrenkrog, B., Koser, J., Schwarz-Herion, K., Deng, J., and Aebi, U. (2007). Nanomechanical basis of selective gating by the nuclear pore complex. Science *318*, 640–643.

Liu, H., Jin, L., Koh, S.B., Atanasov, I., Schein, S., Wu, L., and Zhou, Z.H. (2010). Atomic structure of human adenovirus by cryo-EM reveals interactions among protein networks. Science *329*, 1038–1043.

Lowe, A.R., Siegel, J.J., Kalab, P., Siu, M., Weis, K., and Liphardt, J.T. (2010). Selectivity mechanism of the nuclear pore complex characterized by single cargo tracking. Nature *467*, 600–603.

Lutschg, V., Boucke, K., Hemmi, S., and Greber, U. (2011). Chemotactic antiviral cytokines promote infectious apical entry of human adenovirus into polarized epithelial cells. Nat. Commun. *12*. 10.1038/ncomms1391, 2:391.

Mabit, H., Nakano, M.Y., Prank, U., Saam, B., Döhner, K., Sodeik, B., and Greber, U.F. (2002). Intact microtubules support adenovirus and herpes simplex virus infections. J. Virol. *76*, 9962–9971.

Mahajan, R., Delphin, C., Guan, T., Gerace, L., and Melchior, F. (1997). A small ubiquitin-related polypeptide involved in targeting RanGAP1 to nuclear pore complex protein RanBP2. Cell *88*, 97–107.

Mandelkow, E., and Mandelkow, E.M. (2002). Kinesin motors and disease. Trends Cell Biol. *12*, 585–591.

Martin-Fernandez, M., Longshaw, S.V., Kirby, I., Santis, G., Tobin, M.J., Clarke, D.T., and Jones, G.R. (2004). Adenovirus type-5 entry and disassembly followed in living cells by FRET, fluorescence anisotropy, and FLIM. Biophys. J. *87*, 1316–1327.

Mohr, D., Frey, S., Fischer, T., Guttler, T., and Gorlich, D. (2009). Characterisation of the passive permeability barrier of nuclear pore complexes. EMBO J. *28*, 2541–2553.

Newcomb, W.W., Juhas, R.M., Thomsen, D.R., Homa, F.L., Burch, A.D., Weller, S.K., and Brown, J.C. (2001). The UL6 gene product forms the portal for entry of DNA into the herpes simplex virus capsid. J. Virol. *75*, 10923–10932.

Osmani, A.H., Davies, J., Liu, H.L., Nile, A., and Osmani, S.A. (2006). Systematic deletion and mitotic localization of the nuclear pore complex proteins of Aspergillus nidulans. Mol. Biol. Cell *17*, 4946–4961.

Pante, N., and Kann, M. (2002). Nuclear pore complex is able to transport macromolecules with diameters of about 39 nm. Mol. Biol. Cell *13*, 425–434.

Pasdeloup, D., Blondel, D., Isidro, A.L., and Rixon, F.J. (2009). Herpesvirus capsid association with the nuclear pore complex and viral DNA release involve the nucleoporin CAN/Nup214 and the capsid protein pUL25. J. Virol. *83*, 6610–6623.

Patel, S.S., Belmont, B.J., Sante, J.M., and Rexach, M.F. (2007). Natively unfolded nucleoporins gate protein diffusion across the nuclear pore complex. Cell *129*, 83–96.

Pfister, K.K., Wagner, M.C., Stenoien, D.L., Brady, S.T., and Bloom, G.S. (1989). Monoclonal antibodies to kinesin heavy and light chains stain vesicle-like structures, but not microtubules, in cultured cells. J. Cell Biol. *108*, 1453–1463.

Puntener, D., and Greber, U.F. (2009). DNA-tumor virus entry—from plasma membrane to the nucleus. Semin. Cell Dev. Biol. *20*, 631–642.

Puntener, D., Engelke, M.F., Ruzsics, Z., Strunze, S., Wilhelm, C., and Greber, U.F. (2011). Stepwise loss of fluorescent core protein V from human adenovirus during entry into cells. J. Virol. *85*, 481–496.

Rabut, G., Doye, V., and Ellenberg, J. (2004). Mapping the dynamic organization of the nuclear pore complex inside single living cells. Nat. Cell Biol. *6*, 1114–1121.

Reddy, V.S., Natchiar, S.K., Stewart, P.L., and Nemerow, G.R. (2010). Crystal structure of human adenovirus at 3.5 Å resolution. Science *329*, 1071–1075.

Ribbeck, K., and Gorlich, D. (2002). The permeability barrier of nuclear pore complexes appears to operate via hydrophobic exclusion. EMBO J. *21*, 2664–2671.

Rietdorf, J., Ploubidou, A., Reckmann, I., Holmstrom, A., Frischknecht, F., Zettl, M., Zimmermann, T., and Way, M. (2001). Kinesin-dependent movement on microtubules precedes actin-based motility of vaccinia virus. Nat. Cell Biol. *3*, 992–1000.

Rosa-Calatrava, M., Grave, L., Puvion-Dutilleul, F., Chatton, B., and Kedinger, C. (2001). Functional analysis of adenovirus protein IX identifies domains involved in capsid stability, transcriptional activity, and nuclear reorganization. J. Virol. *75*, 7131–7141.

Rux, J.J., and Burnett, R.M. (2000). Type-specific epitope locations revealed by X-ray crystallographic study of adenovirus type 5 hexon. Mol. Ther. *1*, 18–30.

Sargent, K.L., Meulenbroek, R.A., and Parks, R.J. (2004). Activation of adenoviral gene expression by protein IX is not required for efficient virus replication. J. Virol. *78*, 5032–5037.

Schaack, J., Bennett, M.L., Shapiro, G.S., DeGregori, J., McManaman, J.L., and Moorhead, J.W. (2011). Strong foreign promoters contribute to innate inflammatory responses induced by adenovirus transducing vectors. Virology *412*, 28–35.

Splinter, D., Tanenbaum, M.E., Lindqvist, A., Jaarsma, D., Flotho, A., Yu, K.L., Grigoriev, I., Engelsma, D., Haasdijk, E.D., Keijzer, N., et al. (2010). Bicaudal D2, dynein, and kinesin-1 associate with nuclear pore complexes and regulate centrosome and nuclear positioning during mitotic entry. PLoS Biol. *8*, e1000350. 10.1371/journal.pbio.1000350.

Strawn, L.A., Shen, T., Shulga, N., Goldfarb, D.S., and Wente, S.R. (2004). Minimal nuclear pore complexes define FG repeat domains essential for transport. Nat. Cell Biol. *6*, 197–206.

Strunze, S., Trotman, L.C., Boucke, K., and Greber, U.F. (2005). Nuclear targeting of adenovirus type 2 requires CRM1-mediated nuclear export. Mol. Biol. Cell *16*, 2999–3009.

Suntharalingam, M., and Wente, S.R. (2003). Peering through the pore: nuclear pore complex structure, assembly, and function. Dev. Cell *4*, 775–789.

Suomalainen, M., Nakano, M.Y., Boucke, K., Keller, S., Stidwill, R.P., and Greber, U.F. (1999). Microtubule-dependent minus and plus end-directed motilities are competing processes for nuclear targeting of adenovirus. J. Cell Biol. *144*, 657–672.

Suzuki, Y., and Craigie, R. (2007). The road to chromatin—nuclear entry of retroviruses. Nat. Rev. Microbiol. *5*, 187–196.

Tang, Y., Winkler, U., Freed, E.O., Torrey, T.A., Kim, W., Li, H., Goff, S.P., and Morse, H.C., 3rd. (1999). Cellular motor protein KIF-4 associates with retroviral Gag. J. Virol. *73*, 10508–10513.

Trotman, L.C., Mosberger, N., Fornerod, M., Stidwill, R.P., and Greber, U.F. (2001). Import of adenovirus DNA involves the nuclear pore complex receptor CAN/Nup214 and histone H1. Nat. Cell Biol. *3*, 1092–1100.

van Oostrum, J., and Burnett, R.M. (1985). Molecular composition of the adenovirus type 2 virion. J. Virol. *56*, 439–448.

Watanabe, T.M., Yanagida, T., and Iwane, A.H. (2010). Single molecular observation of self-regulated kinesin motility. Biochemistry *49*, 4654–4661.

Wiethoff, C.M., Wodrich, H., Gerace, L., and Nemerow, G.R. (2005). Adenovirus protein VI mediates membrane disruption following capsid disassembly. J. Virol. *79*, 1992–2000.

Wilkins, C., and Gale, M., Jr. (2010). Recognition of viruses by cytoplasmic sensors. Curr. Opin. Immunol. *22*, 41–47.

Wodrich, H., Cassany, A., D'Angelo, M.A., Guan, T., Nemerow, G., and Gerace, L. (2006). Adenovirus core protein pVII is translocated into the nucleus by multiple import receptor pathways. J. Virol. *80*, 9608–9618.

Woodward, C.L., Prakobwanakit, S., Mosessian, S., and Chow, S.A. (2009). Integrase interacts with nucleoporin NUP153 to mediate the nuclear import of human immunodeficiency virus type 1. J. Virol. *83*, 6522–6533.

Xue, Y., Johnson, J.S., Ornelles, D.A., Lieberman, J., and Engel, D.A. (2005). Adenovirus protein VII functions throughout early phase and interacts with cellular proteins SET and pp32. J. Virol. *79*, 2474–2483.

Zhang, X., Chen, S., Yoo, S., Chakrabarti, S., Zhang, T., Ke, T., Oberti, C., Yong, S.L., Fang, F., Li, L., et al. (2008). Mutation in nuclear pore component NUP155 leads to atrial fibrillation and early sudden cardiac death. Cell *135*, 1017–1027.